View metadata, citation and similar papers at core.ac.uk
brought to you by CORE
provided by CERN Document Server

LHCb–RICH-2006–061

RICH Reconstruction And Particle Identification Using Ring Fit Methods : Standalone PID in the RICH2 Detector

M. Benayoun[(a)], P. David[(a)], L. DelBuono[(a)] , G. Gilles[(a)], Ch. Jones[(b)]

[(a)] LPNHE Paris VI/VII, F-75252 Paris, France

[(b)] Cavendish Laboratory, Madingley Road, Cambridge, CB3 0HE, UK

Version 0.0

November 16, 2006

Abstract

We have extended the ring fit algorithm presented in earlier works, in order to transform it into a fully standalone PID algorithm running over the full RICH2 momentum range. For this purpose, the full information provided by the tracking (track direction and momentum as well as their errors) is accounted for in the minimized χ^2 function along with the photon information. Additionally, all available information concerning the Cerenkov light emission effect is accounted for in the PID algorithm. PID efficiencies and misidentification rates are found similar to the global ID results, while the statistical information is still much more reliable.

1 Introduction

In a previous LHCb note [1], we outlined a PID Algorithm based on Ring Fit Methods (namely, the RichRingRefit Algorithm). As implemented, this algorithm was running as slave of the Global ID algorithm [2], in the sense that photons used to start the iteration procedure of the ring fit are collected within a window[1] opened around the Cerenkov angle value expected from the Global ID assignment. Above some momentum (say 50 GeV/c), this condition is practically unbiasing and safe ; at low momenta, however, the RichRingRefit algorithm might tend to favour the heavy/light flavor choice already provided by the Global ID algorithm.

Within this framework, the RichRingRefit algorithm is nevertheless useful as it allows to supplement the Global ID identification with reliable statistical information not accessible otherwise at the expense of negligible additional CPU time.

Among the reliable statistical information derived from the RingRefit algorithm, the $\pi - K$ separation obtained from fitting the ring reproduces well the momentum dependence expected from the Cerenkov effect theory, while the corresponding result provided by the Global ID algorithm does not and is additionally hard to interpret. Moreover, the fit probability distribution behaves canonically and thus allows one to use probability thresholds meaningfully. Several other examples can be found in Ref. [1] where the statistical properties of the RichRingRefit Algorithm have been thoroughly considered.

There are two limiting conditions in the present use of Ring Fit Methods within the LHCb RICH software :

- The photons used are those associated with the most probable mass assignment, following the Global ID recognition.
- The RichRingRefit Algorithm is implemented for particle identification only in RICH2.

In this note, an algorithm which releases the first constraint is outlined providing an identification performance comparable to that of the Global ID method ; the controlled statistical properties of the former RichRingRefit Algorithm are preserved. It happens that the RICH2 parameter calibration performed with the former RingRefit algorithm remains valid, both methodologically and numerically.

The forthcoming – and final – step will be to extend the recognition to the (gas) RICH1 data with still an unknown performance. Due to the small number of Cerenkov photons and to the large level of background, there is little hope to extend successfully a ring fit method to aerogel data.

Basically, the working of the present version of the Ring Fit Algorithm is the same as those of the former RichRingRefit Algorithm. Therefore, in the present note, we mostly limit ourselves to giving the information specific to the extension of the ring fit method and to the PID decision choice. In some sense, it is a progress report describing the working of an (autonomous) algorithm which can be run independently of any other and can be fully compared to other methods. It is named RichStereoFit Algorithm.

[1] Some $n\sigma$ cut, with σ computed dynamically – see Section **5** in Ref. [1]

2 The RichStereoFit Algorithm

As stated above, the RichStereoFit and the former RichRingRefit algorithms share the same structure. Namely, the first step is to select photons associated with each track under each possible mass assignment ; the second step is basically an iterative procedure aiming at getting the track direction improved under each mass assumption by minimizing some χ^2 ; the changes of the χ^2 are determined by removing candidate photons too far from the expected ring. The last step is to compare the fit results for the five mass assignments and choose a preferred assignment according to criteria to be defined.

In this last step, the distance between the fit angle and the expected angle plays some role. The distribution of photons along the ring and an estimate of the number of (true) Cerenkov photons also contribute to defining the preferred mass assignment.

The first step is exactly the same as those of the former RichRingRefit Algorithm ; we refer the interested reader to Sections **5** and **6** of Ref. [1] for further information. The algorithm parameters currently have exactly the same values as in the RichRingRefit Algorithm and their tuning is performed as described previously in Ref. [1].

2.1 The χ^2 Of The RichStereoFit Algorithm

As in the RichRingRefit Algorithm, the basic input information is provided by the photon and track directions unit vectors. The ring fit methods are local (*i.e.* track by track) methods and the photons considered are supposed to be (candidate) Cerenkov photons emitted by the track along its radiator path.

One then considers a frame where the polar axis is taken along the charged track direction ; all photon direction unit vectors are drawn with their origin at the origin of this frame and with their endpoints all laying on the unit sphere centered at the frame origin. One then performs a stereographic projection of these photon directions onto the equatorial plane of the unit sphere. The projected photon direction endpoints are then expected to be all spread onto a circle with radius $R = \tan(\theta/2)$, where θ is the particle Cerenkov angle [1] and with its center located at the origin.

Let us remind a few notations in order to avoid referring too much to [1] for trivial information. The circle equation is written :

$$f(x,y) = c - x^2 - y^2 + 2ax + 2by \quad , \tag{1}$$

where $c = R^2 - a^2 - b^2$, a and b being the circle center coordinates in the stereo plane. The projected photon coordinates are :

$$x_i = r_i \cos\varphi_i \quad , \quad y_i = r_i \sin\varphi_i \quad , \quad r_i \equiv \tan\frac{\theta_i}{2} \tag{2}$$

where θ_i is the Cerenkov angle of the i^{th} photon and φ_i its azimuth around the cone (the azimuth origin is *a priori* arbitrary).

The tracking provides a reliable information on the track direction (t_x and t_y) and momentum (p). Ref. [1] worked out in details the relation between t_x and t_y on the one hand and a

and b on the other hand. The iterative procedure which underlies the ring fit methods has been simplified by the change of coordinates which moves the image of the track direction in the stereo plane to the origin ($a = 0$ and $b = 0$). In this case $c = R^2$ and the full error covariance matrix of a, b and c can be explicitly derived from known information on a track by track basis.

The random variable defining the error function on the Cerenkov angle can be written [1] :

$$\delta\theta = \delta'\theta + \frac{1}{\tan\theta}\left[\frac{\delta n(\lambda)}{n(\lambda)} + \frac{\delta\beta}{\beta}\right] \tag{3}$$

where $\delta'\theta$ is a random variable which accounts for the errors due to the pixel size, to the choice of the (unknown) emission point along the track trajectory inside the radiator and the track curvature errors. The rest of Equation (3) is derived from the definition of the Cerenkov angle ; $\delta'\theta$ together with the middle term in the Equation just above defines what was named uncorrelated error [1] because these are independent random variables associated with each photon separately. In contrast, the last term, named $\delta\theta_{speed}$ in [1] is common to all photons associated with the same charged track and gives rise to correlations ; it can also be written :

$$\delta\theta_{speed} = \frac{1}{\tan\theta}\frac{\delta\beta}{\beta} = \frac{1}{\tan\theta}\frac{m^2}{E^2}\frac{\delta p}{p} \tag{4}$$

When computing the covariance matrix $V_{ij} =< \delta f_i \ \delta f_j >$ as explained in [1] ($f_i \equiv f(x_i, y_i)$), terms like $< \delta\theta_i \ \delta\theta_j >$ arise and, at leading order in R (which is small –a few tens of milliradians – in both LHCb gaseous radiators), one can write :

$$< \delta\theta_i \ \delta\theta_j >= \sigma_\theta^2\delta_{ij} + \frac{1}{4R^2} < \left[\frac{\delta\beta}{\beta}\right]^2 > g_i g_j \tag{5}$$

where σ_θ^2 is the variance of the uncorrelated errors and g is a vector defined in order to match photon indices[2] ; it is such that $g_i = 1$ for each i. A priori, R should be the true circle radius, but an estimate of it is enough for practical purposes. The content of σ_θ^2 has been widely discussed in [1].

Gathering all these pieces of information, one can show that the photon error covariance matrix is at leading order :

$$\begin{aligned} V_{ij} = \ & R^2\sigma_\theta^2\delta_{ij} + 4R^2[\sigma_a^2 c_i c_j + \sigma_b^2 s_i s_j + \sigma_{ab}(c_i s_j + c_j s_i)] \\ & + \frac{1}{4}\sigma_c^2 g_i g_j + 2R[(c_i g_j + c_j g_i)\sigma_{ac} + (s_i g_j + s_j g_i)\sigma_{bc}] \end{aligned} \tag{6}$$

where c_i and s_i are the sine and cosine of the photon azimuth angle φ_i on the Cerenkov ring. σ_θ^2, σ_a^2, σ_b^2 and σ_{ab} have been widely discussed in [1] ; σ_c^2 is the coefficient of $g g_j$ in Equation (5). The quantities $\sigma_{ac} =< \delta a \ \delta c >$ and $\sigma_{bc} =< \delta b \ \delta c >$ can easily be computed using the random variables δa and δb defined in [1] and $\delta c = R\delta\theta_{speed}/2$; indeed, all other contributions to δc give vanishing correlations.

[2]The second term in Equation 5 is a constant entering each entry of the covariance matrix. Using $g_i g_j (\equiv 1)$ simply allows to preserve the tensor structure.

The photon part of the χ^2 to be minimized is

$$\chi^2_{photons} = \sum_{i,j} f_i V^{-1}_{ij} f_j \tag{7}$$

V^{-1}_{ij} can be derived from Equation (6) on a track by track basis whatever the number of photons. A fast way to perform this inversion is given in the Appendix of [1] ; the most time consuming operation is the inversion of one 3 by 3 matrix which should be performed at each iteration step[3] as described in the Appendix of Ref. [1].

The main change with respect to the previous $\chi^2_{photons}$ function[1] is the occurrence of additional correlation terms in the error covariance matrix (the second line of Equation (6)) related to the track momentum.

Minimizing the $\chi^2_{photons}$ function in Equation (7) is in principle enough to get the best solution for any given assignment. However, if the photons populate a small fraction of the circle (less than, or about, 180°), the fit procedure generally fails [3]. A way to circumvent this difficulty is to supplement the χ^2 with additional information accessible from the tracking. This is done by adding the following term to the χ^2 :

$$\chi^2_{track} = A^t \Sigma^{-1} A \tag{8}$$

as in the RichRingRefit χ^2. However, now, we extend the vector A to $A = (a, b, c - c_0)$ as the measured track direction has been shifted to ($a = 0, b = 0$) and c_0 is the radius squared expected from tracking information ; the error covariance matrix Σ is inherited from the tracking software with σ^2_a, σ^2_b and σ_{ab} modified in order to include multiple scattering effects inside the RICH gas volume. σ_{ac}, σ_{bc} and σ^2_c are purely derived from tracking information. c_0 in the third component of the vector A is $\tan\theta/2$ as coming from the momentum value and the current mass assignment (recall that we examine now the five possible mass assignments in turn).

Therefore, the quantity to be minimized in the iteration procedure becomes :

$$\chi^2(a, b, c) = \sum_{i,j} f_i V^{-1}_{ij} f_j + A^t \Sigma^{-1} A \tag{9}$$

The difference between the present version of the algorithm and the former one is the use of a "measured" value for c which follows from having a good measurement of the track momentum and the five possible mass assignments in turn.

As we previously allowed the mass assignment to change (with respect to the starting Global ID best solution), we did not include the constraint provided by the present c terms in Equation (9) in the former RichRingRefit Algorithm. In the present release, as we first examine the five possible mass assignments independently of each other, it is perfectly legitimate to include this strong constraint into the fit procedure[4].

In the RichRingRefit Algorithm, the χ^2 had $n_\gamma - 1$ degrees of freedom, while this is presently equal to the number of photons surviving the iterative cleaning up procedure, n_γ.

[3] Note an unfortunate misprint in Equations (54) : the minus sign in the last equality should be removed.

[4] As a first attempt, we tried the previous release of the fit algorithm – *i.e.* without the *c* terms – running on the five possible mass assignments. The results, while interesting, were not as good as those presently achieved.

Therefore, having only one (surviving) photon, would not prevent to have a quality factor like the fit probability ; provisionally however, we maintain a minimum number of 4 photons in order to assert that we really observe a ring. This implies some tiny efficiency loss near the Cerenkov threshold (and/or for low geometrical acceptance rings).

2.2 Use of the Fit Probability Information

The result of the fit performed through the minimization of the χ^2 given by Equation (9) is an improved track direction, the best circle radius (*i.e.* the Cerenkov angle) and the error covariance matrix of these quantities. For each track, five fits are performed by assuming the five possible mass assignments[5].

Leaving free a and b has a clear motivation : the tracking information provides the track direction at the RICH2 entrance window. However, because of the material of the RICH2 detector and of the fringe field in the detector volume, the information provided by the tracking concerning the track direction (and thus the circle center) has certainly to be improved ; the fit procedure is supposed to perform the change from the track direction at the radiator volume entrance window to some averaged track direction inside the radiator volume. So, having a_{fit} and b_{fit} different from the values provided by the tracking can be legitimately expected.

Instead, for obvious physical reasons, c_{fit}, the best fit value returned for c by the ring fit, should stay consistent with the value c_0 derived from knowing the momentum p with the appropriate mass assignment (*i.e.* the mass assignment corresponding to the fit under consideration), if the mass assignment is correct.

Therefore, for each of the five fits, two pieces of information are relevant :

- The probability Pr(ringFit) associated with $\chi^2(a_{fit}, b_{fit}, c_0)$,
- The probability Pr(θ_C) of the pull :

$$\mathrm{Pull}_C = \frac{c_{fit} - c_0}{\sigma_c} \quad . \tag{10}$$

The former information Pr(ringFit) gives the ring fit probability given the Cerenkov angle expected for the expected mass assignment for the best track direction, the latter Pr(θ_C) gives the distance of the Cerenkov fit angle to the one expected for this particular fit. It is indeed clear that an angle fit value θ_{fit} returned by the fit which would be inconsistent with the expected value should be disfavored, whatever the fit quality value Pr(ringFit).

Even if these two pieces of information (Pr(ringFit) and Pr(θ_C)) somewhat overlap, they are independent of each other to a large extent. Practically, we assume their mutual independence.

As there is a minimum number of starting photons (4 by default) in order to initiate the fit procedure, it may happen that fits associated with some given assignments are not performed. Quite generally this figure happens when the mass assignment corresponds to a particle below

[5] Actually, of course, a fit is performed for a given assignment only if one is above the corresponding Cerenkov threshold.

(or very close to) the Cerenkov threshold ; in this case the corresponding fits are simply not performed[6].

Pr(ringFit) and Pr(θ_C) are the most important elements for the best ID decision, however other pieces of information are also helpful and discussed below.

3 Additional Information About Cerenkov Rings

There are two more properties of the Cerenkov Effect which are of some relevance in PID procedures. Cerenkov photons are expected to be uniformly distributed in azimuth around the track direction and the average number of emitted Cerenkov photons has to be consistent with theoretical expectations.

3.1 The Worst Empty Arc

The Cerenkov photons generated by a track should be uniformly distributed in azimuth along the Cerenkov cone, and, hence, along the ring in the stereo plane. However, Cerenkov photons associated with a given track mix with those associated with neighbouring tracks in azimuth. Therefore the uniform distribution property should be handled with some care. Indeed, even if the Cerenkov photons associated with neighbouring tracks follow a uniform distribution, they might provide local accumulations on the ring produced by the track under consideration. Therefore, on real data, observed photon hits are generally not uniformly distributed along a given ring.

In addition, acceptance effects in the detector HPD plane can generate large areas where Cerenkov photons are undetected ; this effect produces arcs between consecutive photons which can be large compared to expectations, as illustrated by the last Figure 9 in [1]. This is also shown in the present Figure 1, where large empty arcs on the Cerenkov ring are clearly associated with small ring acceptances. Additionally this plot proves that ring acceptances are always significantly smaller than 1, as one observes an upper bound slightly larger than 80%.

There is however, an interesting property of uniform distributions which keeps still some use, even in a noisy environment. It can be derived from the following theorem [4] :

- Theorem (induced partition) :
  n independently and randomly chosen points $X_1, \ldots, X_n$ partition the interval $[0,1]$ into $n+1$ intervals whose length L has a common distribution given by ;

$$\Pr(L > t) = (1-t)^n \quad , \quad 0 < t < 1 \tag{11}$$

- This theorem obviously applies to $n+1$ ordered points uniformly and randomly distributed on a circle with the arc lengths ($[X_1, X_2]$,... $[X_i, X_{i+1}]$, etc ...) normalized (*i.e.* $t = [X_i, X_{i+1}]/2\pi$). One has only to cut the circle at the $(n+1)^{th}$ point to get back to the $[0,1]$ interval and to the conditions of the theorem above.

[6]There is no point in attempting below threshold recognition until a conclusion on RICH1 data handling is reached.

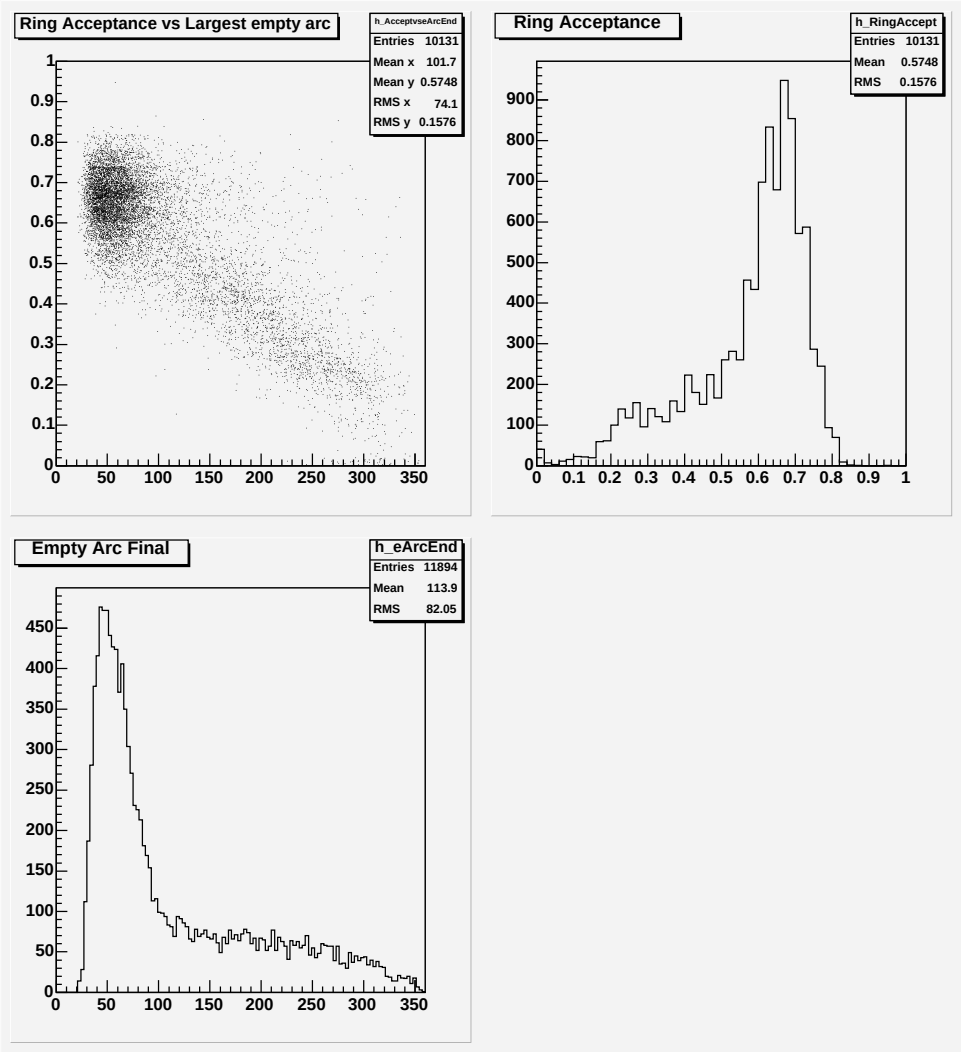

Figure 1: *Ring acceptance in the HPD plane versus largest empty arc in DC04 data. Acceptance and arc distributions are obtained by the appropriate projections of the scatter plot (top left figure).*

The Cerenkov light emission is, for each track, uniform in azimuth ; therefore, for tracks isolated in direction, we are in the conditions of the theorem above. However, in the conditions of LHCb, each track has several tracks close in azimuth, giving hits which break this uniformity property. Therefore, one cannot fully use this theorem.

However, a property survives background and acceptance effects. The largest possible empty azimuthal[7] arc on the Cerenkov ring due to acceptance effects is $2\pi(1-a)$, denoting by a the acceptance value ($0 < a < 1$). This is certainly the most pessimistic estimate of the largest empty arc on a ring ; indeed, simulating photon emission around a ring regularly

[7]This includes the HPD dead areas.

by steps of, say, one degree turns out to assume that all non–accepted photons (*i.e.* hitting a HPD plane in inactive areas) are consecutive ; this is clearly not the most common figure as a Cerenkov ring generally overlaps more than one HPD.

On the other hand, n_C, the average number of Cerenkov photons emitted by a track, is proportional to $< \sin^2\theta_C >$ with a calibration constant (generally denoted LN_0 as in [1]) which can be inferred from technical information ; a finer tuning using Monte Carlo truth information can be performed and has provided an average $LN_0 = 4\ 10^4$ for RICH2 DC04 data, with a precision of about 0.25 %.

Therefore, an estimate of the most pessimistic (*i.e.* largest) empty arc A_{max} on the Cerenkov ring can be proposed[8] :

$$A_{max} = 2\pi(1-a) + 2\frac{2\pi}{n_C} \tag{12}$$

When analyzing photons associated with a given track under a given assignment, one identifies the largest observed arc A_{obs} and estimates the number of observable (true) Cerenkov photons to an_C. Then, the theorem given above allows to define the probability $\Pr(\mathrm{worstArc}) \equiv \Pr(A_{obs} > A_{max})$:

$$\Pr(\mathrm{worstArc}) = \begin{cases} \left(1 - \dfrac{A_{max}}{2\pi}\right)^{an_C} & A_{obs} > A_{max} \\ 1 - \left(1 - \dfrac{A_{max}}{2\pi}\right)^{an_C} & A_{obs} \leq A_{max} \end{cases} \tag{13}$$

Following from Figure 1, one certainly has $a < 1$ and the number of photons in the exponent is smaller than the generated one by at least $\simeq 20\%$; so there is no point in over-subtracting the photon number by one unit in order to stay consistent with the theorem.

This probability is an important tool in the proposed ring ID.

As stated above, the worst largest (empty) arc, derived from the acceptance value, assumes that all $non - accepted$ photons are consecutive and this is certainly an incorrect statement in general, as the non–accepted part of the ring should generally not be continuous. Generating Cerenkov photons regularly in azimuth –with, say, one degree steps– and keeping track of the accepted ones, it is possible to access the actual largest empty arc on the ring with a good precision. It happens that this true largest empty arc does not lead to improvements compared to using only the acceptance information carried by A_{max}. So, we give up using it, saving this way CPU time.

3.2 Estimating Signal And Background Photons

The ring acceptance a for a track under a given assignment can be derived using a standard tool of the RICH package (*i.e.* the RichGeomEffPhotonTracing class). Then, the average number of *observed* signal photons n_A can be derived :

[8] If there were no acceptance effect, the average angular distance between two consecutive photons would be $2\pi/n_C$; if there is a hole in the acceptance, assuming that one Cerenkov photon falls inside this hole, the average angular distance may become twice this mean value. Then, for an acceptance much below 1, Equation (12) looks a reasonable estimate. For practical purposes, we prevent n_C in this Equation to be smaller than a minimum of 4.

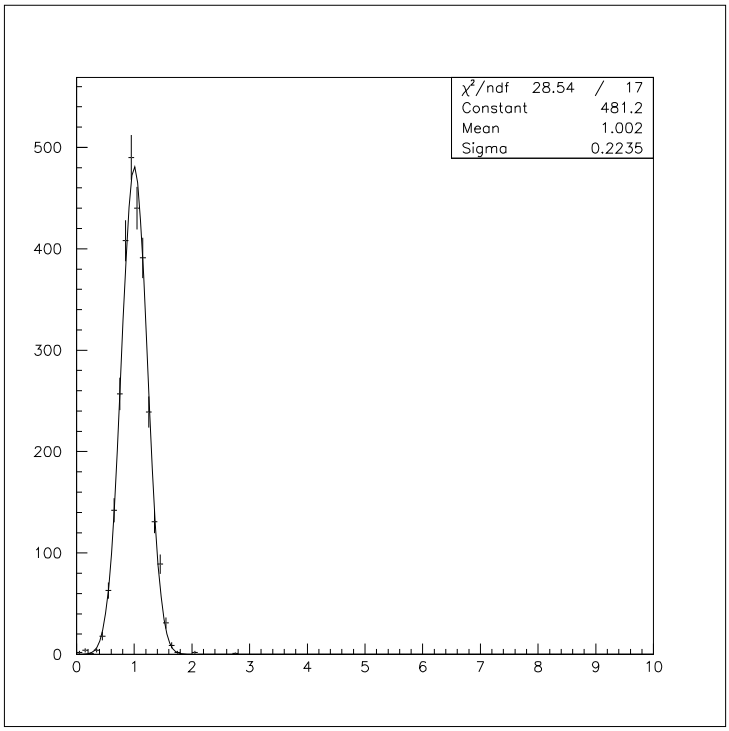

Figure 2: *Ratio of n_C defined in Equation (14) and the number of Monte Carlo photons associated with the track in DC04 data.*

$$n_A = a\, n_C = a\, LN_0 < \sin^2\theta_C > \tag{14}$$

with good accuracy, as the accuracy on the acceptance is well under control. Figure 2 shows the distribution of the ratio n_A to the actual number of (observed) Monte Carlo photons associated with the track considered. The distribution behaves like a Gaussian with a mean quite consistent with 1 when LN_0 in Equation 14 is taken at $4\ 10^4$, and using the ring by ring acceptance[9]. The standard deviation of this distribution reflects the Poisson nature of Cerenkov light emission.

However, mostly due to neighboring tracks, there is a non–negligible background contamination in the photon set associated with a given track at the end of the iterative ring fit procedure.

It is likely that true signal (Cerenkov) photons are Gaussian distributed around the ring radius. Instead, background photons have *a priori* an unknown distribution ; we make the assumption that their distribution is uniform in some interval around the ring radius. Additionally, photons surviving the fit are all located, at most, at 3 σ from the ring radius[1]. Therefore, under our assumption, counting only photons located at better than 1.28 σ of the ring, one keeps 80% of the (Gaussian) signal while keeping only 43 % of the (flat) background hits. As it is

[9]The quantity named LN_0 in [1] was guessed to be around $2.2 \div 2.5\ 10^4$, using essentially technical information on RICH2 [5]. Instead of $4\ 10^4$ just quoted, which is free of ring acceptance effects, the value $2.2 \div 2.5\ 10^4$ actually accounts for an averaged acceptance $< a >$. The average acceptance of the plot shown in Figure 1 is $< a >= 0.58$

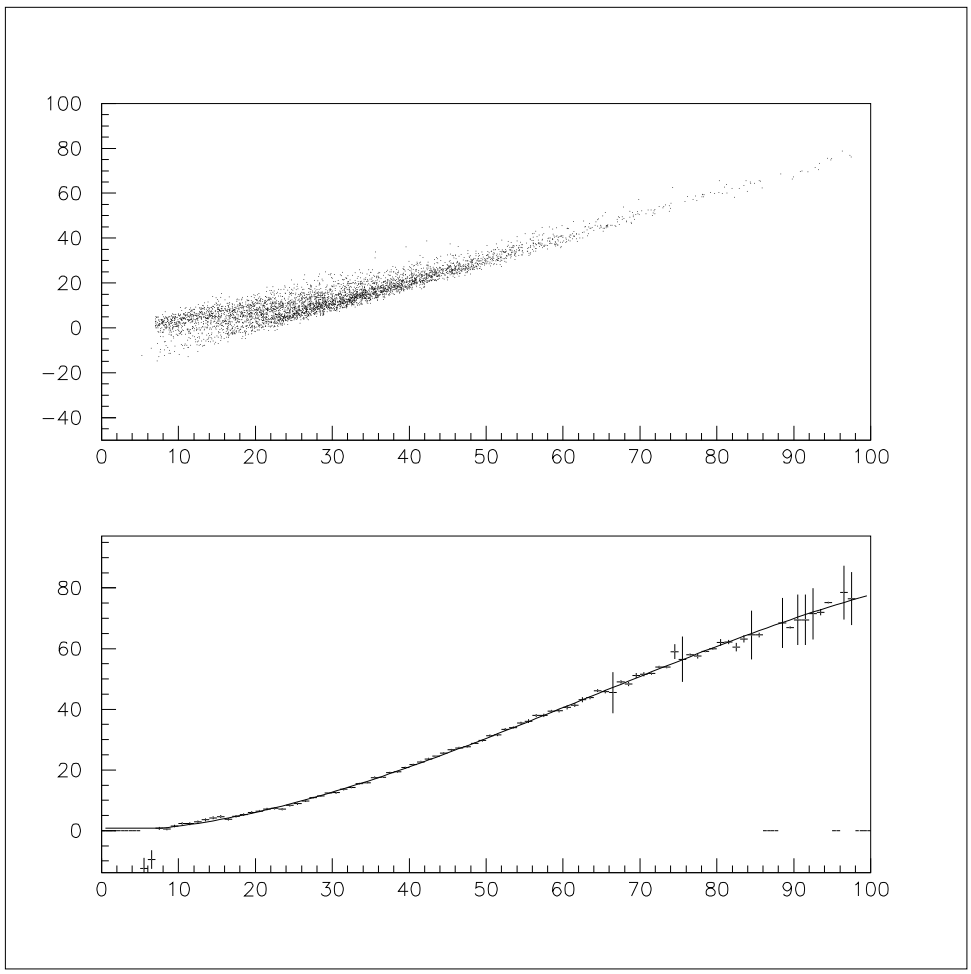

Figure 3: *Background estimate as a function of the number of photons located within* 1.28σ *of the ring (80% probability).*

better to have to estimate the smallest possible photon background yield, this interval of 1.28 σ on both sides of the ring allows to keep most of the signal while removing about 60% of the background.

Then, an estimate of the background yield within 1.28σ around the ring radius is given by the difference between $n_\gamma(1.28\sigma)$ – the number of photons surviving the fit and located within 1.28 σ of the ring – and 0.8 n_A (see Equation (14)) – the average number of expected signal photons in the same interval ($\pm 1.28\sigma$). The upper Figure 3 shows this estimate of the background photon yield n_{bkg} versus $n_\gamma(1.28\sigma)$; the lower Figure 3 shows, superimposed, the profile and a spline fit of it. This spline fit clearly represents a reasonable parametrization of the background yield as a function of $n_\gamma(1.28\sigma)$. This is confirmed by Figure 4 ; here, the difference between :

$$n_{signal} = n_\gamma(1.28\sigma) - n_{bkg} \quad , \tag{15}$$

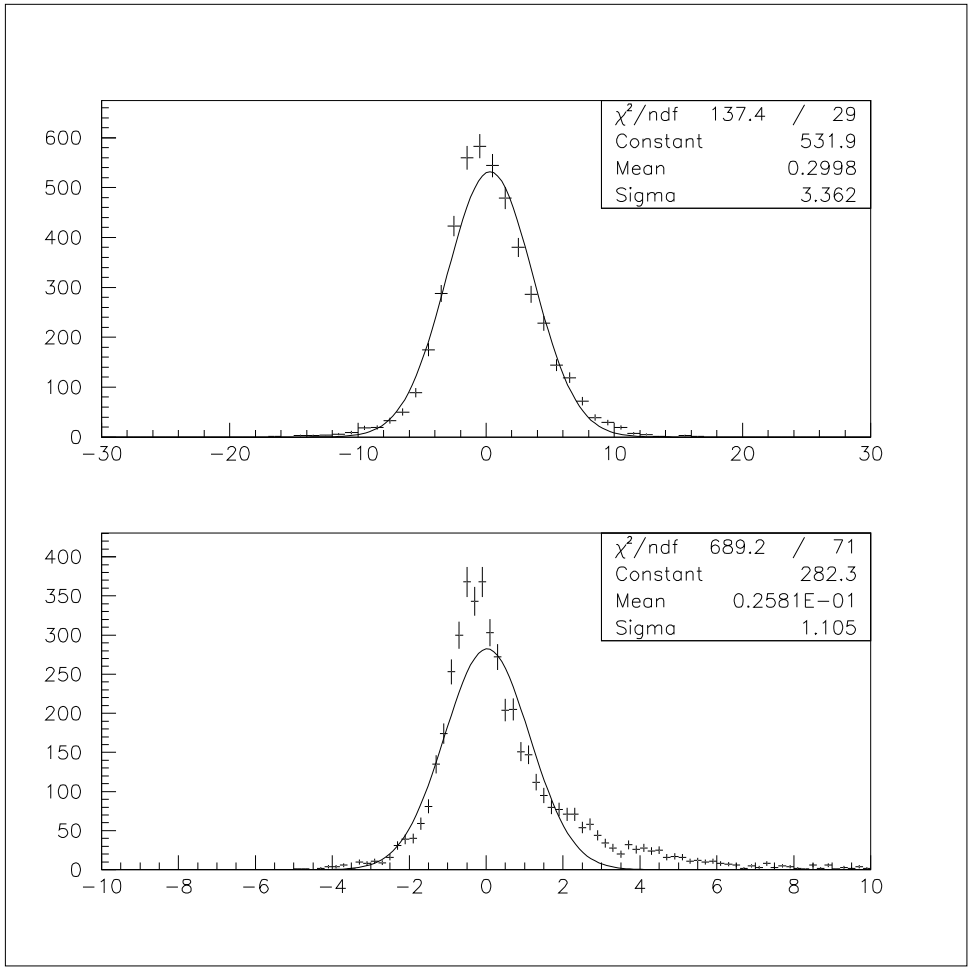

Figure 4: *Residual (milliradians) and pull of the number of observed true Cerenkov photons located on the ring within* 1.28σ.

our estimate of the photon signal yield, and[10] $0.8n_{MC}$, *i.e.* the residual, looks reasonably Gaussian and is well centered ; the lower Figure 4 shows the ratio of this residual to $\sqrt{0.8n_A}$, *i.e.* the pull, assuming the error is Poisson–like. This pull clearly departs from Gaussian but looks nevertheless acceptable.

The probability of this pull Pr(n_{signal}) is thus considered as another relevant piece of information.

[10] n_{MC} is the number of true Monte Carlo photons as given in the DST for the track considered. It can be considered as sampled out of a Poisson distribution of mean n_A. $0.8n_A$ is an estimate of the Monte Carlo signal photon yield within $\pm 1.28\sigma$ of the ring.

4 The Best ID Decision

As a summary, we have defined 4 probabilities for each track under each possible mass assignment :

- Pr(ringFit), the ring fit probability,
- Pr(θ_C), the probability of the fit Cerenkov angle compared to the expected one,
- Pr(worstArc), the probability of the largest arc between photons consecutive in azimuth,
- Pr(n_{signal}), the probability of the estimated Cerenkov photon yield within the photons surviving the ring fit iteration procedure.

Pr(ringFit), Pr(θ_C) and Pr(n_{signal}) have the usual shape expected from a χ^2 probability, *i.e.* a flat distribution with a peak located around zero probabilities as illustrated by the first three distributions shown in Figure 5. Instead, Pr(worstArc) is a two–peak distribution, one located around zero probabilities, the other located toward unit probabilities ; this is illustrated by the distribution in Figure 5d. This two–peak structure reflects an expected property : the largest observed arc on a ring is either favored or disfavored with little room for intermediate situations.

The desirable criterion to define the best (ring) ID should correspond to the assignment for which the product :

$$\{\ [\mathrm{PIDCriterion}]\ ::\quad \mathrm{Pr(ID)}\ =\ \mathrm{Pr(ringFit)} * \mathrm{Pr}(\theta_\mathrm{C}) * \mathrm{Pr(worstArc)} * \mathrm{Pr}(n_{signal})\ \} \tag{16}$$

is the largest. At low momenta, the value of Pr(worstArc) frequently suppresses the probability of some assignments compared to others for the same track. This is a pure geometric effect : at low momenta, the ring radii are much better separated than at high momenta ; in this case, the largest empty arc on the ring can vary significantly from one assignment to the other.

This criterion basically determines our decision choice. However two remarks which will be expressed below affect the practical use of this criterion.

4.1 Threshold Probabilities

It happens sometimes that one among the probabilities defined in Section **3** lies in the zero probability peak region for several assignments, while all other probabilities share the same order of magnitude. In this case, the relevant question is to what extend the precise value of this $\simeq$ zero probability should be trusted ? or, stated otherwise, whether the precise numerical value of a very low probability should have a decisive role in the mass assignment choice.

In order to invetigate the problem, we show in Figure 6 the low probability peak structure for each of the relevant probabilities. This clearly shows that very small probabilities have a range of several orders of magnitude. What happens with some frequency is that all probabilities except for one (say, Pr(worstArc) for illustrative purpose) are of the same order of

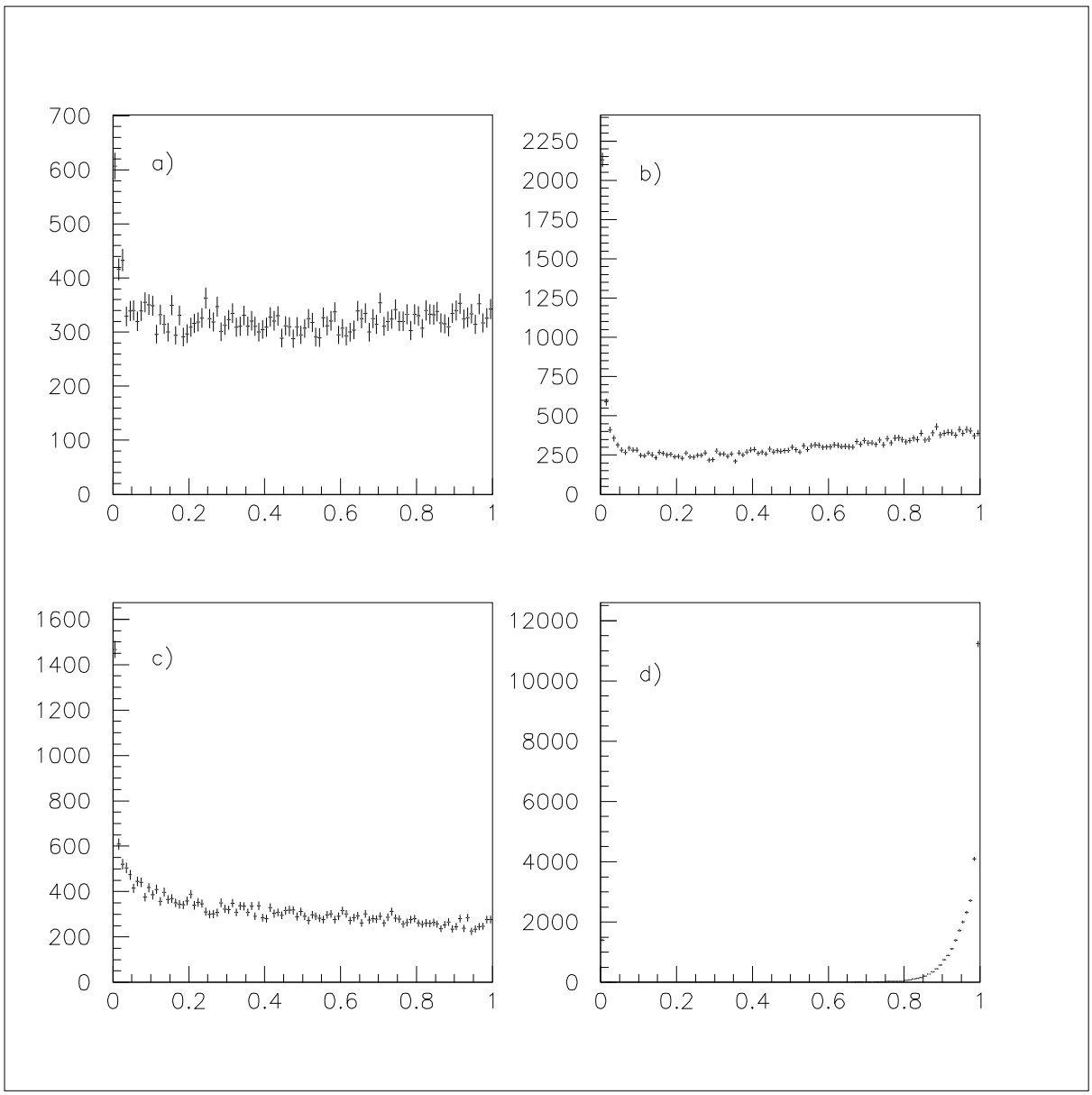

Figure 5: *Probability distributions for the MCTruth assignment. a) Probability of the fit Cerenkov angle. b) Probability of the estimated (true) Cerenkov photons yield. c) Ring fit probability. d) Probability of the largest arc on the Cerenkov ring ; note, for this plot that there are two peaks.*

magnitude. Now, if for two different assignments we have, for instance, Pr(worstArc) = 10^{-6} and 10^{-10} respectively, the PID criterion defined above will definitely favor the former against the latter, whatever is the value of the rest of the product. Taking into account the approximations performed, one could consider that this is an undesirable drawback.

In order to circumvent this problem, we have introduced a threshold probability : If all

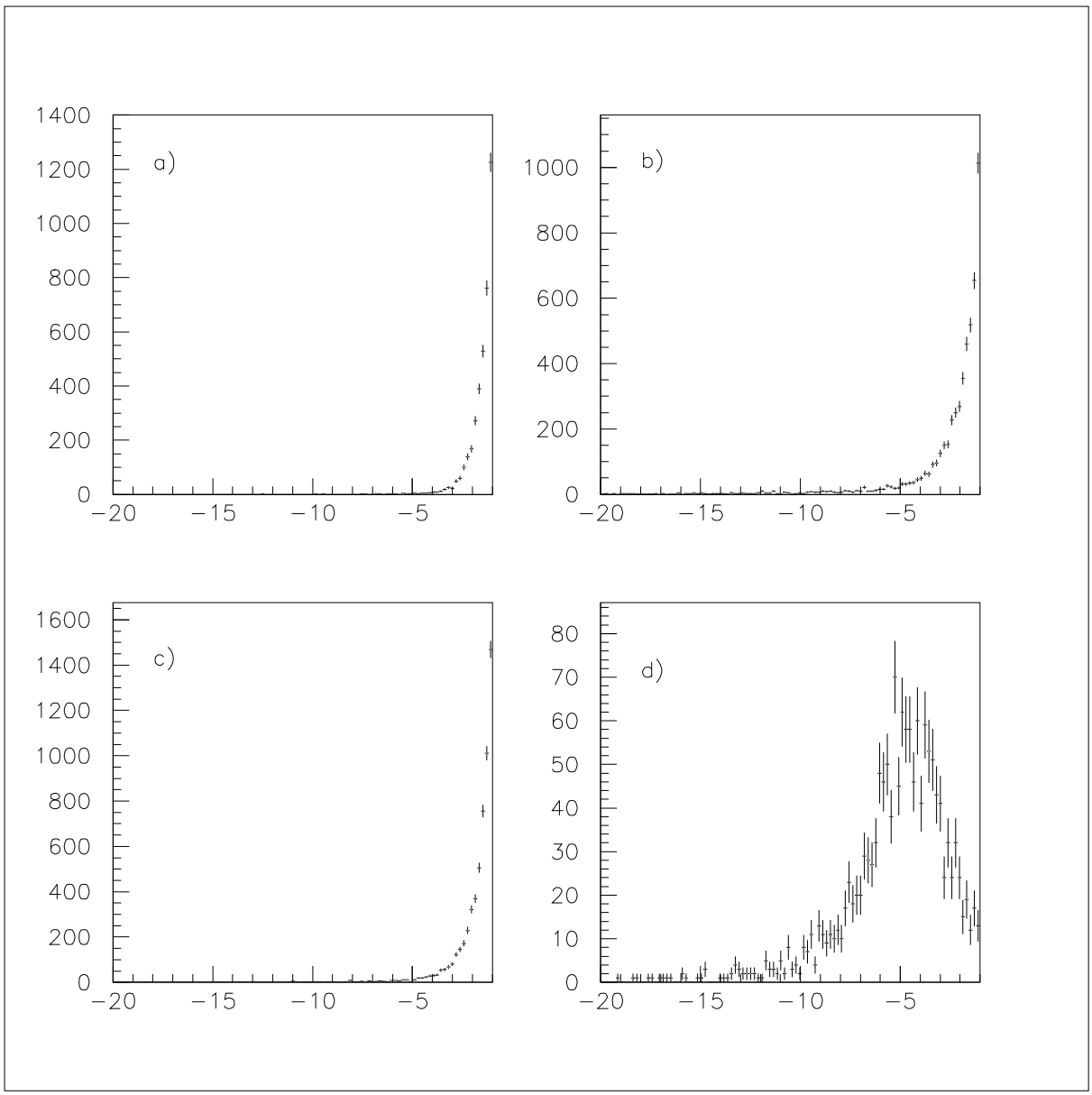

Figure 6: *Low value region of the probability distributions. The information plotted is the decimal logarithm of each probability. a) the (decimal logarithm) probability of the fit Cerenkov angle. b) the (decimal logarithm) of the estimated Cerenkov photons yield probability. c) the (decimal logarithm) of the ring fit probability. d) the (decimal logarithm) of the largest arc probability.*

assignments for which a fit has been obtained have one given probability always below some threshold, this probability is removed from the PID criterion. For the different probabilities, we have set this threshold to a common value ($\Pr(x) = 10^{-3}$) ; obviously, this is equivalent to introducing a minimum probability.

One may note that threshold value can be different for different probability kinds and that the precise values can be chosen somewhat smaller without influencing dramatically the PID performance.

4.2 Unambiguous Photon Yield, The UPY Criterion

Another situation appears with a noticeable frequency and should be handled with some care ; this is when some probability products are numerically very close to each other. The kind of situation[11] is when the two largest probabilities are, for instance, 10% and 12% for which one naturally chooses the latter, while clearly the former is as well justified.

So, below some threshold, uneasy to fix numerically, choosing the largest probability product (even corrected as stated in the Subsection just above) is doubtful. If we had exhausted all the available information, this would nevertheless be the most appropriate choice[12].

However, there is still one piece of information which has not been used : The unambiguous photon yield for a track. Indeed, in the LHCb environment, most of background hits found when examining the photon populations along the possible rings associated with a given track are mostly signal photons of tracks close in azimuth to the track considered. Therefore, an interesting piece of information is whether a given photon appearing as associated with one track under a given mass assignment is also associated with other tracks. If not, such a photon is called unambiguous, otherwise it is classified ambiguous.

After a first pass, examining all possible assignments for all tracks, one determines for each track and each assignment how many of its photons have also been associated with other tracks by the ring fit procedure. One may infer that the assignment for a track which has the largest number of photons not associated with other tracks is the right assignment.

Practically, for each track, one keeps the two best assignments following from the criterion defined above and selects as PID the one which corresponds to the largest unambiguous photon yield. For equal unambiguous photon yields, one selects the assignment associated with the largest value of the PID criterion defined above. We name this procedure, the unambiguous photon yield (UPY) criterion.

In Figures 7 and 8 the PID performance of the ring fit algorithm using or not the UPY criterion are shown. In order to get these plots, one has used only RICH2 data.

For sake of completeness : one defines the efficiency for light particles as the ratio of the number of particles identified as light among the light particles (relying on the MC truth) to the number of generated light particles. Purity is defined as the number of reconstructed light particles among generated light particles divided by the number of particles reconstructed as light ; misidentification is 1 - purity. Mutatis mutandis, the corresponding definitions for heavy particles can be derived.

The effect of the UPY criterion is clear : the efficiency curve for light assignment is sharply improved, especially at high momentum (*i.e.* above 100 GeV/c). Instead, the heavy assignment

[11] Of course, this is a general issue, not specific of the ring fit approach.

[12] Actually, one could consider complex objects consisting each of a track with "weighted" mass assignments ; even if statistically grounded, this way to proceed is not of common use. This might become rapidly hard to handle and one generally prefers using each track with one assignment and correct globally for misidentification.

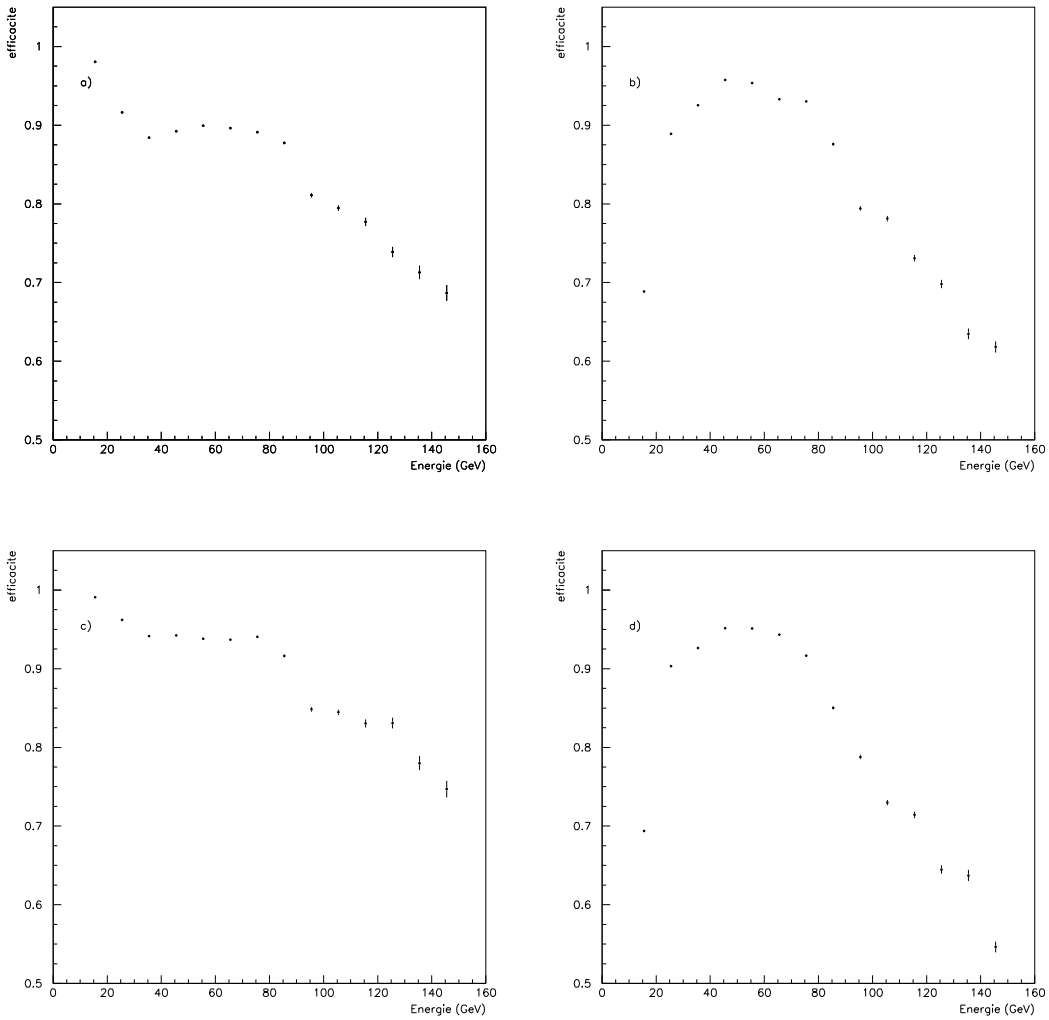

Figure 7: *Efficiency distributions when using the ring fit method. a) Efficiency for e,μ,π without using the UPY criterion, b) efficiency for K,P without using the UPY criterion, c) efficiency for e,μ,π using the UPY criterion, d) efficiency for K,P using the UPY criterion.*

is slightly degraded at high momenta (*i.e.* above 100 GeV/c) while its misidentification rate is significantly improved over the whole momentum range. Keeping in mind that the 3 σ separation is around 110 GeV/c on average [1], one can consider that the UPY criterion should indeed be included in the PID decision process[13].

[13]Indeed, this limit around 110 GeV/c is the actual limit RICH2 3 σ $\pi - K$ separation. Above this value, whatever is the performance and whatever is the algorithm, the RICH performance actually does not rely on the RICH system angular resolution.

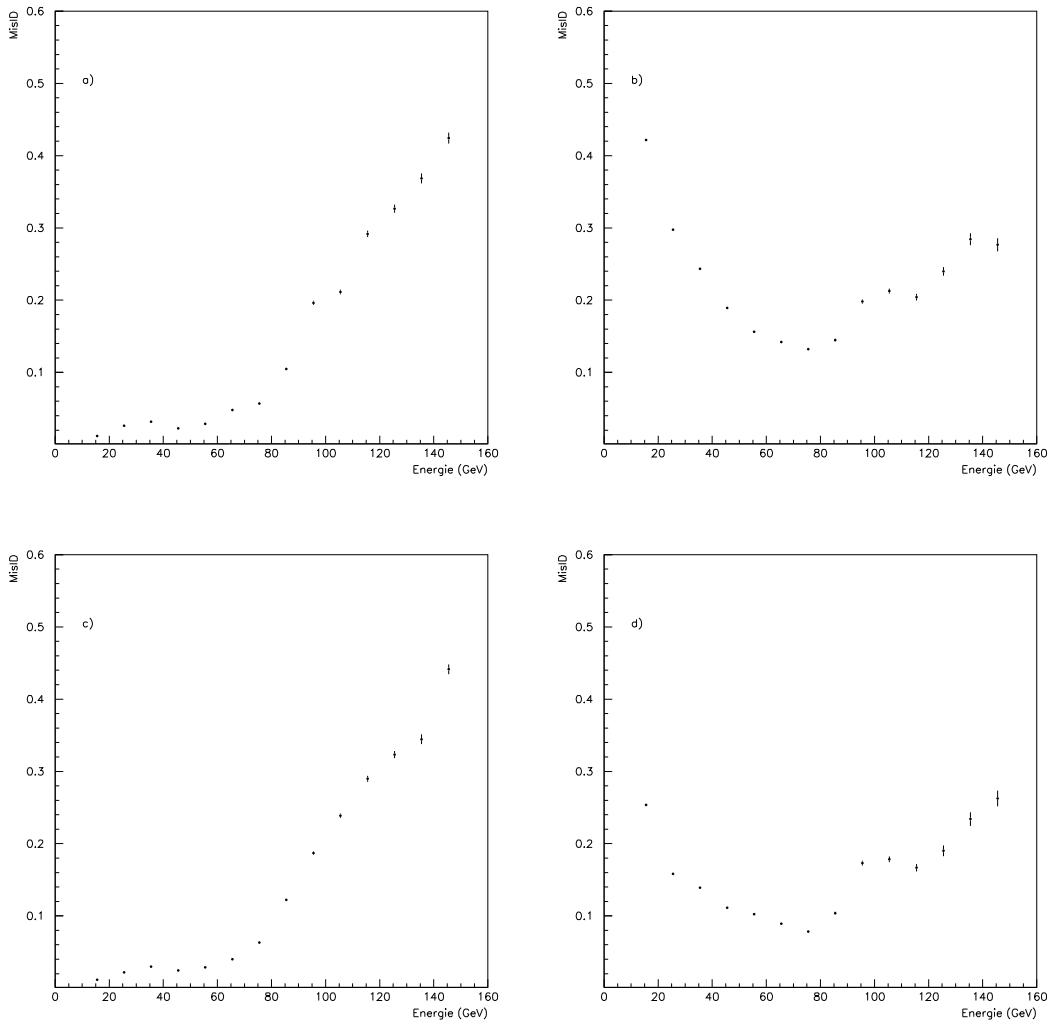

Figure 8: *Misidentification distributions when using the ring fit method. a) misidentification for e,μ,π without using the UPY criterion, b) misidentification for K,P without using the UPY criterion, c) misidentification for e,μ,π using the UPY criterion, d) misidentification for K,P with RingID using the UPY criterion.*

5 PID Performance

The Ring Fit identification performance can now be fully compared with the performance of the Global ID algorithm. Figure 9 shows the efficiency distribution of both algorithms for heavy and light assignments. The difference of efficiencies for each kind of particles (light or heavy) is also shown. Clearly, the efficiency for light particles is better at high momentum for the ring fit algorithm, while the efficiency for heavy is better at high momentum for the Global ID algorithm. Efficiencies below, say 80 GeV$/c$, are alike for both algorithms.

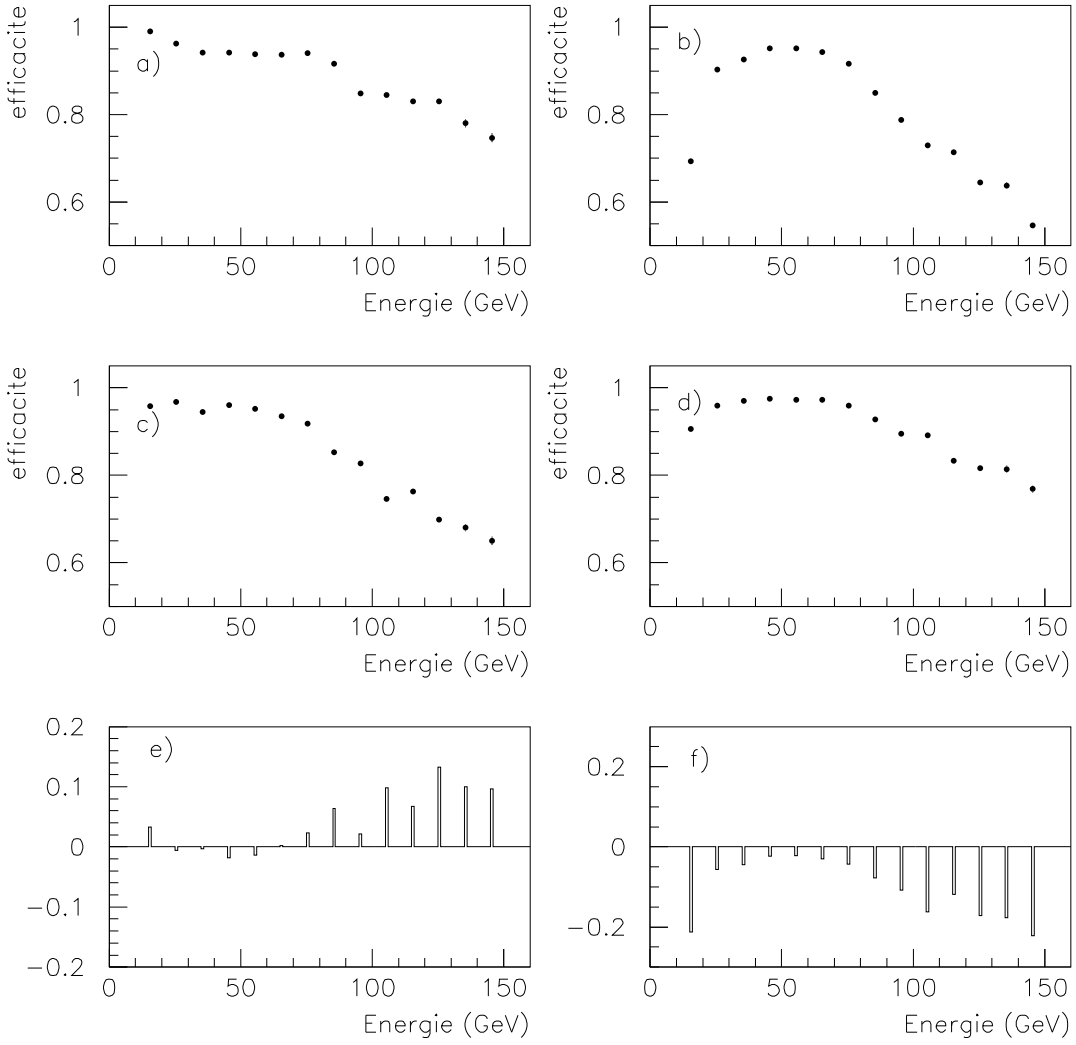

Figure 9: *Left side distributions are efficiencies for e,μ,π identification with the RingFit and GlobalID algorithms, Right side distributions are efficiencies for K, P identification with the RingFit and GlobalID algorithms. a) efficiency for e,μ,π with RingFit. b) efficiency for K, P with RingFit. c) efficiency for e,μ,π with GlobalID. d) efficiency for K, P with GlobalID. e) difference between a) and c). f) difference between b) and d).*

Figure 10 displays the corresponding misidentifi cation distributions. For light particles, the RingFit algorithm exhibits a larger misidentifi cation rate at high momentum, reflecting its larger effi ciency. Instead, the misidentifi cation rate for heavy particles are alike over the whole momentum range, except at the Cerenkov threshold where, the minimum number of photons

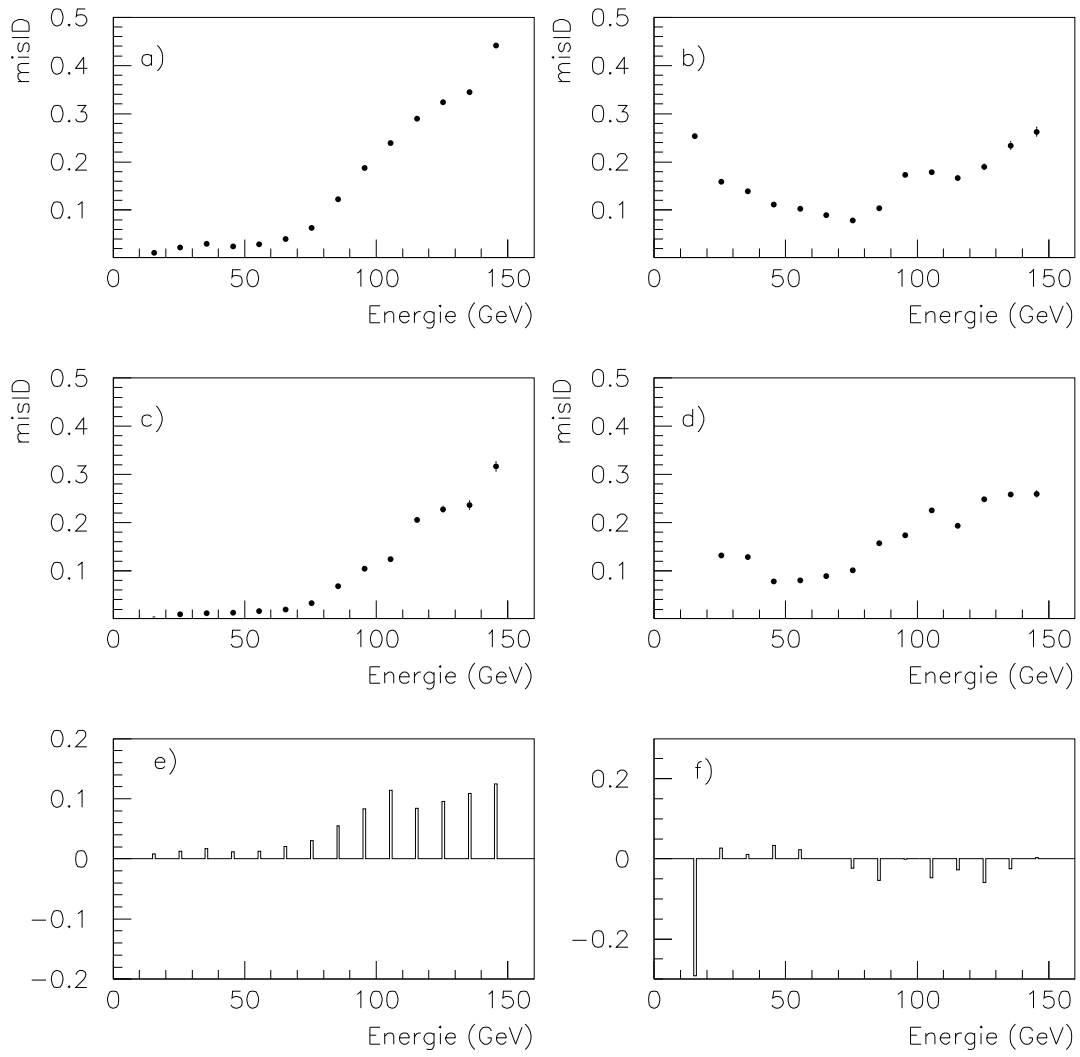

Figure 10: *Left side distributions are misidentification rates for e,μ,π with RingFit and GlobalID algorithms. Right side distributions are misidentification rates for K, P with RingFit and GlobalID algorithms. a) misidentification for e,μ,π with RingFit. b) misidentification for K, P with RingFit. c) misidentification for e,μ,π with GlobalID. d) misidentification for K, P with GlobalID. e) difference between a) and c). f) difference between b) and d).*

(4) requested in order to perform the ring fi t plays certainly a large role.

6 Conclusions

We have successfully extended the ring fit procedure for RICH2 data in order to get a standalone algorithm, able to perform particle identification over the whole momentum range covered by this counter. The ring fit and global ID algorithms exhibit similar identification performance while the statistical information carried by the ring fit algorithm is much better under control and reliable. Running on only RICH2 data, the computing times for both algorithms are similar.

The ring fit procedure now includes all information actually relevant to the Cerenkov effect : ring fit probability, Cerenkov angle probability, largest observed arc on the Cerenkov ring (accounting for acceptance effects and uniform distribution), estimation of the number of signal photons, estimation of unambiguous photon yield. Additionally, each of these probability distributions has its expected shape (flat in general or peaked for the special case of the largest arc on the Cerenkov ring).

Most of the difference between the algorithms is concentrated in the high momentum region where (see [1]) the statistical information carried by the global ID algorithm still remains to be understood.

The next step is to extend the procedure in order to include RICH1 data. This study is presently under way.

Acknowledgements

We gratefully acknowledge Roger Forty (Cern) for useful comments and reading the manuscript.

References

[1] M.Benayoun and Ch. Jones, “RICH Reconstruction And Particle Identifi cation Using Ring Fit Methods : Application to the RICH2 Detector”, LHCb-RICH–2004–057, Jan. 2005.

[2] R. Forty and O. Schneider, “Rich Pattern Recognition”, LHCb/98–040, RICH, 30 April 1998.

[3] M. Benayoun, L. DelBuono and Ph. Leruste, “Reconstruction and Particle Identifi cation For A DIRC system”, Nucl. Inst. Meth. **A 426** (1999) 283.

[4] W. Feller, “An Introduction to Probability Theory and Its Applications”, John Wiley, New York 1971, second edition, Volume II, page 21.

[5] ”LHCb RICH”, Technical Design Report CERN/LHCC/2000–0037, LHCb TDR 3, 7 September 2000.